Both whole cell and acellular pertussis vaccines are now available against pertussis infection. The whole cell pertussis vaccine is composed of a suspension of formalin-inactivated *B. pertussis* cells. In contrast, the acellular pertussis vaccine contains purified, inactivated components of *B. pertussis* cells. Acellular pertussis vaccines now in use contain primarily pertussis toxin (PT) and filamentous hemagglutinin [3]. Pertussis vaccines cause local reactions, such as pain, redness, or swelling, in 20–40% of treated children, and systemic events, such as fever of 105 °F or higher, febrile seizures, and hypotonic–hyporesponsive episodes, have been reported [4]. The Japanese Ministry of Health Labour and Welfare reported that the adverse reactions, such as fever, pain, edema, and purpura, were observed in 237 people in 5.4 million vaccine-treated people in 2003.

While the mechanisms underlying adverse reactions remain unknown, vaccines should undergo extensive safety and efficacy tests to control vaccine quality. Fundamental is the assurance that any vaccine destined for public use is manufactured under Good Manufacturing Practices (GMP) and has passed appropriate pre-release lot testing for purity and potency, for which manufacturers must submit samples of each vaccine lot and their own test results. In Japan as in other countries, all the vaccines must conform to the "Minimal Requirement of Biological Products" and are obliged to pass national control tests [5].

Pertussis vaccine toxicity causing adverse reactions, is evaluated by the conventional animal toxicity tests, which are based on the peripheral white blood cell (WBC) counts in mice after subcutaneous or intra-peritoneal injection [6,7]. In mice, PT blocks extravasation reactions that mediate lymphocyte homing from peripheral blood to solid lymphoid tissues [8,9]. For a vaccine to be considered safe, an increase in the WBC count in mice should not exceed 0.5 LPU (leukocytosis promoting unit)/ml at day 3 after injection [5]. Pertussis vaccine toxicity is also typically assessed by the histamine sensitization test. In this test, mouse rectal temperatures are monitored after histamine challenge on the fourth day of vaccine injection [10]. To develop more sensitive and more reproducible methods, we undertook comprehensive gene expression analysis of rats after administration of the pertussis vaccine by using DNA microarrays [11]. Hybridization of labeled nucleic acid from a sample to the microarrays identifies genes expressed in the specific sample. This approach allows simultaneous analysis of expression of the multiple genomes in a single cycle experiment. This approach has already been used for evaluation of side effects of drugs [12].

2. Materials and methods

2.1. Animals

Male Wistar rats (8 weeks) were obtained from SLC (Tokyo, Japan). All animals were housed in rooms maintained at 23 ± 1 °C, with 50 ± 10% relative humidity, and 12-h light:12-h dark cycles at least 1 week prior to the test challenge. Rats typically weighed 160–200 g on arrival.

2.2. Vaccines and toxin

Reference pertussis vaccine (reference vaccine; RE) was a lyophilized whole cell preparation of pertussis organisms incompletely inactivated by formaldehyde, used for National Quality Control Tests on pertussis vaccine in Japan since 1981. It was reconstituted in 12 ml of physiological saline, and 5 ml were injected intra-peritoneally (IP). PT (pertussis toxin) are prepared and purified by ammonium-sulfate fractionation and sucrose density gradient centrifugation, and treated with formaldehyde to destroy the toxic activity, and added with aluminum salt. PT (Wako Chemicals, Osaka, Japan) and PV (a generous gift of The Chemo-Sero-Therapeutic Research Institute, Kumamoto, Japan) were adjusted to 5 μg/ml (PT concentration). RE, PV, and different concentrations of PT were injected into rats IP (5 ml/rat). Five milliliters of saline (SA) were injected as a control.

2.3. WBC counts

A leukocytosis-promoting test was performed according to the Minimum Requirements of Biological Products [5]. Ten microliters of each blood samples were used for WBC counting. The count was performed with a Z1 coulter particle counter (Beckman Coulter, Fullerton, CA). Three rats per group were treated by RE, PT, PV, and SA, and were analyzed on day 1–4 post-treatment. The experiments were performed three times.

2.4. Histology

Vaccine-treated livers were harvested from rats and fixed in Bouin's Solution (Sigma, St. Louis, MO) and 4% (w/v) paraformaldehyde at 4 °C for 48 h. After fixation, tissues were dehydrated through a series of graded alcohols and xylene and embedded in paraffin. Chilled paraffin blocks were cut into 4–6 μm sections, which were floated onto glass slides and dried overnight and stained with Hematoxylin and eosin (HE) and periodic acid Schiff (PAS). Cellular polysaccharide deposits were detected using the PAS reaction. Three rats per group were treated by RE, PT, PV, and SA, and were analyzed on day 1–4 post-treatment. The experiments were performed twice. Immunohistochemical staining was carried out as described [13]. Briefly, after blocking with 3% BSA in PBS, 4 μm sections were incubated overnight with anti-α1-acid-glycoprotein (Agp) (AgriSera, Vännäs, Sweden) at 4 °C overnight. Signals were detected with a VECTASTAIN ABC Kit (Vector Laboratories, Inc., Burlingame, CA). Nuclei were stained with hematoxylin.

In situ hybridization was performed essentially as described [14]. *In situ* hybridization using liver sections was carried using digoxygenin (DIG)-labeled RNA probes specific for *Agp* (Genebank accession number

NM053288, 0.77 kb) and *Hpx* (NM053318, 1.48 kb). All cRNA probes were generated from the corresponding coding sequences. *Agp* forward primer: 5-tgcacatggttcttgtcgtt-3, reverse primer; 5-gaatcgaggtgcacaggagt-3, *Hpx* forward primer; 5-cgctactactgcttccaggg-3, reverse primer; 5-atgctgttcactttctgggg-3. *In situ* hybridization with the antisense or sense probes was incubated at 42 °C for 24 h in a humidified chamber. Hybridized DIG-labeled cRNA was detected using AP labeled-anti-DIG mouse fab fragments (Roche Diagnostics, Lewes, UK). The sections were treated with BCIP/NBT and mounted in Gel mount (Biomeda, Foster City, CA). Three rats per group were treated by RE, PT (5 μg/ml), PV, and SA, and were analyzed on day 1–4 post-treatment. The experiments were performed twice.

2.5. RNA preparation

Rats were sacrificed to obtain the lateral left lobe of the liver. Organs were immediately frozen in liquid nitrogen for storage. Thawed tissue was homogenized and mixed with an ISOGEN reagent (NIPPON GENE, Tokyo, Japan). Total RNA was prepared from the lysate in accordance with the manufacturer's instructions. Poly(A)+RNA was prepared from total RNA with a Poly(A) Purist Kit (Ambion, Austin, TX), according to the manufacturer's instructions.

2.6. Microarray preparation and expression profile acquisition

For the microarray analysis, three rats per group were treated by RE, PT (5 μg/ml), PV, and SA, and livers from each group were analyzed on day 1–4 post-treatment. Totally 48 liver samples were analyzed for this experiment.

A set of synthetic polynucleotides (80-mers) representing 11,464 rat transcripts derived from 10,490 independent genes and including most of the RefSeq clones deposited in the NCBI database (MicroDiagnostic, Tokyo, Japan) was arrayed on aminosilane-coated glass slides (Type I; Matsunami, Kishiwada, Japan) with a custom-made arrayer [15,16]. Poly(A)+RNA (2 μg) was labeled with SuperScript II (Invitrogen, Carlsbad, CA) and Cyanine 5-dUTP for each sample or Cyanine 3-dUTP (Perkin-Elmer, Boston, MA) for a rat common reference RNA (MicroDiagnostic). Labeling, hybridization, and washes of microarrays were performed with a Labeling & Hybridization Kit (MicroDiagnostic) according to the manufacturer. The rat common reference RNA was purchased as a single batch and labeled as an aliquot with Cyanine-3 for a single microarray side by side with each sample labeled with Cyanine-5. Hybridization signals were measured using a GenePix 4000A scanner (Axon Instruments, Whipple Road Union City, CA) and then processed into primary expression ratios ([Cyanine 5-intensity obtained from each sample]/[Cyanine 3-intensity obtained from common reference RNA], which are indicated as 'median of ratios' in GenePix Pro 3.0 software (Axon Instruments)). Normalization was performed for the median of ratios (primary expression ratios) by multiplying normalization factors calculated for each feature on a microarray by the GenePix Pro 3.0 software.

2.7. Data analysis

Data processing and hierarchical cluster analysis were performed using Excel (Microsoft, Redmond, WA) and a MDI gene expression analysis software package (MicroDiagnostic). The primary expression ratios were converted into $\log_2$ values ($\log_2$ Cyanine-5 intensity/Cyanine-3 intensity) (designated log ratios) and compiled into a matrix (designated primary data matrix). To predict the most obvious differences obtained from cluster analysis of the primary data matrix, we extracted genes with $\log_2$ ratios over 1 or under −1 in at least one sample from the primary data matrix and subjected them to two-dimensional hierarchical cluster analysis for samples and genes. To identify genes demonstrating significant changes in expression, we undertook the following: (i) mean averages of $\log_2$ ratios were calculated for each gene from data sets of day 1 SA- and RE-treated samples; (ii) standard deviations were calculated for each gene; (iii) the difference in mean averages between day 1 SA- and RE-treated samples was calculated for each gene and divided by the sum of the corresponding standard deviation values. A value of the difference of the mean averages/the sum of the standard deviations was defined as an expression signal/noise index for each gene. We chose the top 150 genes exhibiting the highest expression signal/noise indexes and extracted expression data corresponding to the 150 genes from the primary data matrix for all the samples, which was subsequently subjected to two-dimensional hierarchical cluster analysis for samples and genes.

2.8. Quantitative RT-PCR analysis

Total RNA was used to synthesize first strand cDNA using a First-strand cDNA Synthesis Kit (Life Science, Inc., St. Petersburg, FL), according to the manufacturer's instructions. Expression levels of Agp and Hpx were analyzed by quantitative (Q) reverse transcriptase–polymerase chain reaction using a 7500 Fast Real-Time PCR System (Applied Biosystems, Foster City, CA) with 7500 Fast System SDS Software Version 1.3. cDNA was amplified for Q-PCR using SYBR Green I (Molecular Probes, Inc.) to detect PCR product. One microliters of six-fold diluted cDNA was used in a 20-μl final volume reaction containing 10 μl SYBR Green® PCR Master Mix (Applied Biosystems), 0.2 μM Agp fwd primer (5′-GCTGGAGCTGGAGAAGGAGACT-3′), and 0.2 μM Agp rev primer (5′-ACAGTCCCCGGAGTTCAGAGA-3′). The 7500 Fast System was programmed to run an initial polymerase activation step at 95 °C for 10 min followed by 40 cycles of denaturation (95 °C for 15 s) and extension (60 °C for 1 min), and product synthesis was monitored at the end of the extension step of each cycle. The same conditions were used with primers 0.05 μM Hpx

fwd (5′-CTGCCTCAGCCCCAGAAAGT-3′) and 0.05 μM Hpx rev (5′-GGGTGGGCTGGGCTAATTC-3′). Agp and Hpx values were normalized against rat β-actin (0.1 μM fwd 5′-ACCGTGAAAAGATGACCCAGATC-3′; rev 5′-GACCAGAGGCATACAGGGACAAC-3′).

2.9. Western blot analysis

One day after treatment, livers were rapidly removed from diethylether anesthetized rats, washed in PBS, and weighed. After dicing, tissue was homogenized in PBS containing protease inhibitors and lysed in PBS containing protease inhibitors, 1% (w/v) Nonidet P-40, 0.5% (w/v) deoxycholate, 0.1% (w/v) SDS, and 10 mM Na-EDTA. Supernatants were collected after centrifugation at 10,000 × *g* for 20 min and used as a whole liver lysate. Fifty micrograms of the lysate was subjected to SDS-PAGE (10% acrylamide) and the separated proteins were transferred to an Immobilon-P membrane (Millipore, Watford, UK). After incubation in TBS (20 mM Tris–HCl (pH 8.0) and 100 mM NaCl) containing 5% (w/v) BSA, the membrane was incubated with anti-AGP (AgriSera) or anti-actin (Santa Cruz Biotechnology, Santa Cruz, CA) antibodies for 1 h and further incubated with HRP-conjugated anti-goat or anti-rabbit IgG. Peroxidase activity was visualized with a LAS 3000 bioimaging analyzer (Fuji Film, Tokyo, Japan).

2.10. Statistical analysis

To evaluate the statistical significance of the difference in expression level of Agp and Hpx, the Student's *t*-test was used to calculate the *P*-value.

3. Results

3.1. Vaccine-treated rats demonstrated leukocytosis in peripheral blood

Animals were treated with 5 ml of reference pertussis vaccine (RE), purified pertussis vaccine (PV), pertussis toxin (PT), or saline (SA), and the peripheral WBCs were counted at days 1, 2, 3, and 4. RE is an incompletely inactivated whole cell vaccine for the reference of PT toxicity. PT is a purified pertussis toxin. To evaluate dose-response to PT, mixture of a constant amount of PV and varying amount of PT, 0.2, 1.0, and 5.0 μg/ml were used for injection (coded as PV + PT0.2, PV + PT1, and PV + PT5, respectively). Three rats per group were analyzed in each day after sample injection. RE-treated rats started to show leukocytosis at day 2; the leukocyte count continued to increase reaching values three times higher than the baseline at day 4 (Fig. 1). PV + PT5-treated rats also demonstrated leukocytosis, as did RE-treated rats. By contrast, PV- and SA-treated animals showed normal WBC counts. WBC counts of both PV + PT0.2- and PV + PT1-treated rats were within the normal range.

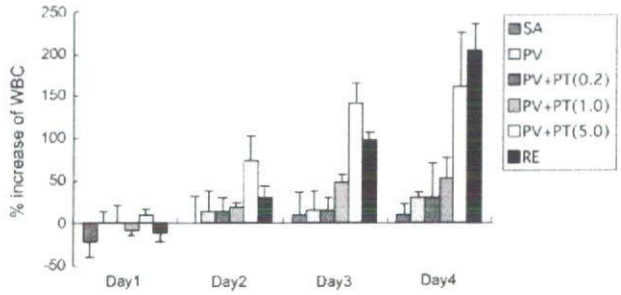

Fig. 1. Leukocytosis-promoting activity in RE- and PT-treated animals. The effects of RE-, PT-, PV-, SA-treatment were analyzed by leukocytosis-promoting tests. Various PT concentrations (0.2–5.0 μg/ml) were added to PV and a WBC count was performed at days 0, 1, 2, 3, and 4. Changes in WBC count are indicated by the mean increase ± S.D. of three independent experiments. Each value was compared to the corresponding control SA.

3.2. Histological analysis in vaccine-treated rats

To analyze the effect of pertussis vaccine on rat liver, we performed histological study on day 1–4 post-treatment twice. As shown in Fig. 2, SA-, PV + PT-, and RE-treated livers showed no significant change in HE stained sections. Since periodic acid Schiff (PAS)-positive glycogen granules in hepatocytes are sensitive to strong stresses by drugs, toxic agents, starvation, and hypoxic conditions, PAS staining was also evaluated. At day 1, we have remarkable change in RE samples by PAS staining, however we could not detect the same change in other samples (Fig. 2). The same results that only RE affect the PAS staining in the hepatocyte were confirmed in the other time point (day 2–4, data not shown). These findings indicated that histological analysis could be useful to monitor toxicity effects induced by RE vaccine, but did not reflect toxicity induced by PT when added to PV.

3.3. Microarray assay of vaccine-treated liver

To evaluate the effect of pertussis vaccine on the gene expression in the liver, we prepared three rats per group. RE-, PT- (5 μg/ml), PV-, and SA-treated groups were sacrificed to take liver samples each at days 1, 2, 3, and 4. Total 48 independent liver tissue samples were analyzed. We labeled poly(A) + RNA purified from the samples and from a rat common reference RNA with Cyanine-5 and Cyanine-3, respectively. Next, we hybridized them to microarrays representing 11,464 transcripts derived from 10,490 independent genes including most of the RefSeq clones deposited in the NCBI database. Hybridization signals were processed into expression ratios as $\log_2$ values (designated $\log_2$ ratios) and compiled into a matrix designated as the primary data matrix (see Section 2). To extract genes whose expression levels altered specifically to RE-administration at day 1 from the primary data matrix, we conducted the statistical operations described in Section 2. When the cluster analysis for liver samples was performed, two large clusters were obtained, and

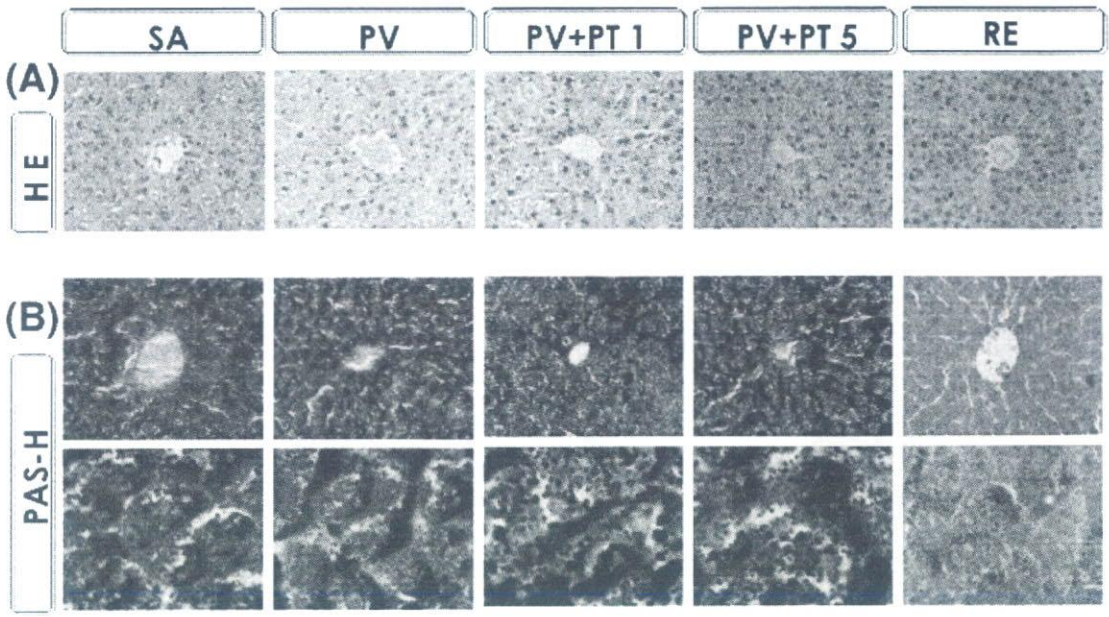

Fig. 2. Histochemical study of RE- and PT-treated liver. The left lobes of sample treated liver were sectioned and stained with HE and PAS. (A) RE-, PV-, PV + PT1- (PT 1.0 μg/ml), PV + PT5- (PT 5.0 μg/ml), and SA-treated liver were stained with HE. (B) Sectioned samples were stained with PAS plus HE and analyzed at low (upper panel) and high (lower panel) magnification.

RE-treated samples (1 day after RE administration, RE/1d) showed cluster different from others (Fig. 3A). We identified top 150 genes exhibiting the highest scores whose expression was either increased or decreased by RE-administration at day 1 (RE-1d in Fig. 3B). Of those genes, 61 are related to metabolism, 21 encode signal transduction molecules, and the rest are classified as toxic response-, inflammation-, and human-disease-related genes (Fig. 3C). Functions of about one-third of these150 genes are unknown.

3.4. Identification of toxicity-specific genes

To identify toxicity-related genes from the microarray data, we compared results from RE-treated samples with SA-treated ones. Agp, S100a8, Phyh, Got1, Lbp, and Hpx genes showed the greatest increase in expression level in RE-treated samples (Table 1). When PT-treated animal samples were compared with PV-treated ones, expressions of Hpx, Acmsd, Tat, and Cyp8b1 were significantly increased (Table 1). Phyh, Got1, Acmsd, Tat, and Cyp8b1 participated in metabolism. On the other hand, Agp, S100a8, Lbp, and Hpx participated in inflammation. To quantify expression of candidate genes, the liver cDNAs were analyzed by quantitative RT-PCR (Fig. 4, lower panel), and compared with the microarray data (Fig. 4, upper panel). Liver cDNA were prepared from two or three rats, and two independent quantification experiments were performed. Agp and Hpx genes demonstrated high expression in RE- and PT-treated liver, and their expression was low in PV- and SA-treated liver (Fig. 4). Both were then chosen for further quantitative analysis.

3.5. Agp and Hpx expression in the liver

For confirmation, we performed *in situ* hybridization and immunohistochemistry. Specific probes against Agp clearly detected Agp mRNA in RE-treated liver at day 1 (Fig. 5G and H). Western blot analysis of the cell lysates showed markedly increase of AGP expression in RE-treated liver in comparison with SA-treated liver (Fig. 5Q). Strong AGP protein expression was also detected in RE-treated livers in comparison to SA-treated livers (Fig. 5R–U). From these data, we conclude that AGP is induced in liver by RE-treatment. Since there is no appropriate antibody against rat Hpx, we analyzed Hpx expression by *in situ* hybridization. Hpx expression was rapidly induced in hepatocytes following RE-treatment, and its expression pattern was similar to Agp (Fig. 5I–P). Thus, of the nine genes identified by microarray analysis, histological analysis with specific RNA probes and antibodies demonstrated the highest correlation with Agp and Hpx. Thus, we identify Agp and Hpx as toxicity-related genes and suggest that these genes could be used as biomarkers.

3.6. Detection of PT activity using Q-PCR analysis

To detect alterations in Agp and Hpx gene expressions after vaccine-treatment, we injected various concentrations of PT (0.008–5.0 μg/ml) and RE into rats. Three rats per group were analyzed. As shown in Fig. 6, expression of Agp and Hpx was tremendously high in RE-treated livers, and both genes showed a strict dependence on the concentration of PT. These genes were clearly up-regulated by PT at

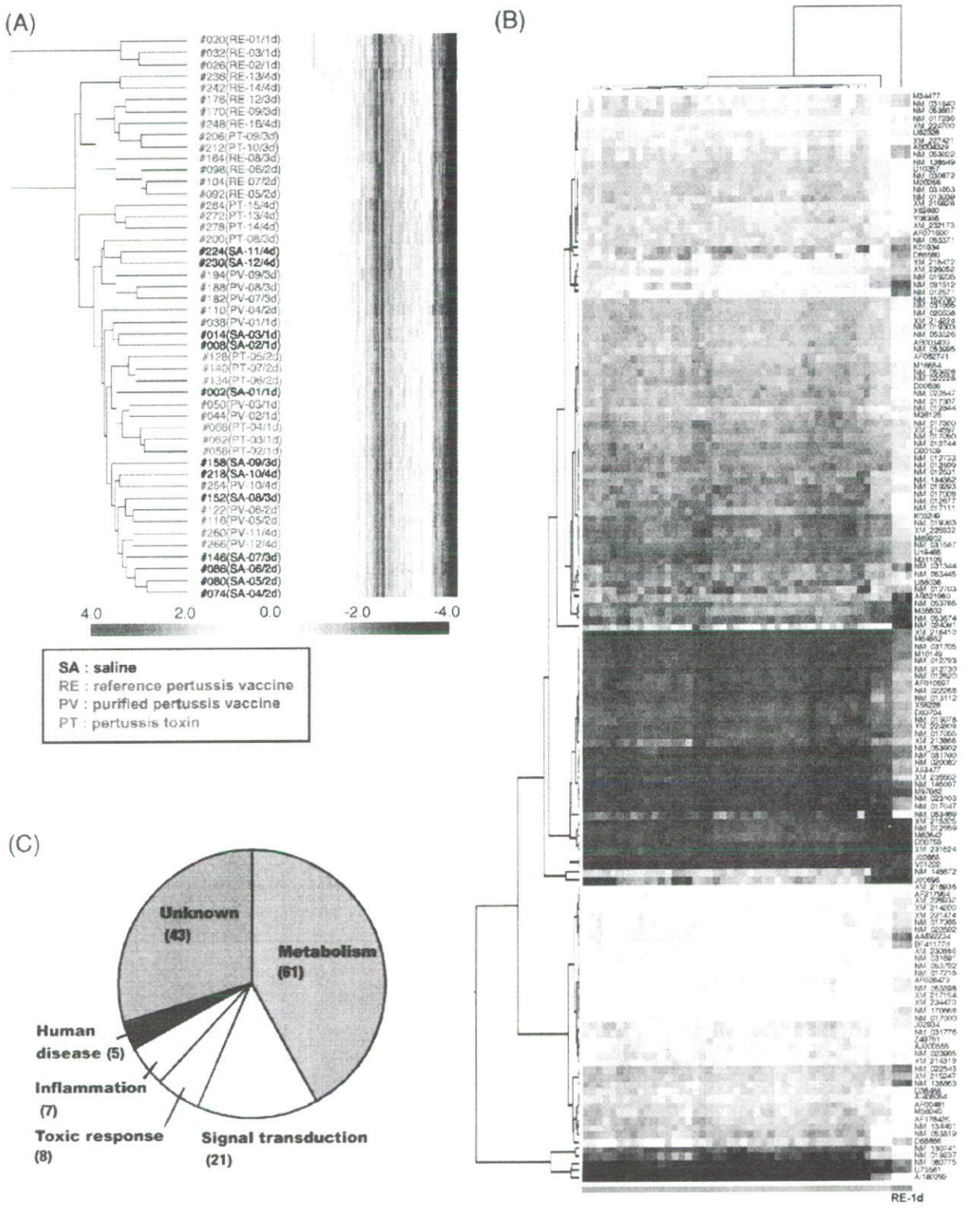

Fig. 3. Gene expression profiles obtained from RE-, PT-, PV-, and SA-treated rats. (A) Genes expressed in sample-treated liver are assembled in the order obtained from the results of cluster analysis. The color bar at left shows the expression ratio *vs.* the common reference RNA in $\log_2$; red and blue indicate increases and decreases in the expression ratio, respectively. (B) One hundred and fifty genes represented showed significant alterations in RE-treated liver at day 1 (RE-1d). The expression pattern of the 150 genes in other samples (pink bar) showed a clear difference from RE-1d (green bar). The *y*-axis of the dendrogram depicts the Euclid square distance as the dissimilarity coefficient. Red and blue indicate increases and decreases in the expression ratio, respectively. (C) Genes are classified in the circle graph.

Table 1
Transcripts upregulated in RE- and PT-treated samples

Accession no.	Symbol	Definition	Molecular function	Expression ratios			
				SA	PV	PT	RE
AB018596	Cyp8b1	Rattus norvegicus mRNA for sterol 12-alpha hydroxylase, complete code	Metabolism	1.76 ± 0.15	1.86 ± 0.48	2.70 ± 0.40	3.61 ± 0.96
J00696	Agp/Orm1	Rat alpha1-acid glycoprotein (AGP) mRNA, complete cds	Inflammation	1.34 ± 0.67	1.58 ± 0.36	4.11 ± 0.38	6.30 ± 0.17
M62642	Hpx	Rat (clone pRHx1) hemopexin mRNA, complete cds	Inflammation	2.74 ± 0.37	2.82 ± 0.15	4.08 ± 0.23	5.30 ± 0.07
NM_012571	Got1	Rattus norvegicus glutamate oxaloacetate transaminase 1 (Got1), mRNA	Metabolism	0.11 ± 0.34	0.18 ± 0.24	1.12 ± 0.35	2.86 ± 0.53
NM_012668	Tat	Rattus norvegicus tyrosine aminotransferase (Tat), mRNA	Metabolism	2.55 ± 0.16	2.34 ± 0.58	3.06 ± 0.41	4.18 ± 0.55
NM_017208	Lbp	Rattus norvegicus lipopolysaccharide binding protein (Lbp), mRNA	Inflammation	1.49 ± 0.24	1.47 ± 0.18	3.59 ± 0.41	4.84 ± 0.17
NM_053674	Phyh	Rattus norvegicus phytanoyl-CoA hydroxylase (Phyh), mRNA	Metabolism	2.03 ± 0.19	2.08 ± 0.12	3.22 ± 0.37	3.78 ± 0.16
NM_053822	S100a8	Rattus norvegicus S100 calcium binding protein A8 (calgranulin A) (S100a8), mRNA	Inflammation	−5.94 ± 0.03	−5.89 ± 0.23	−5.25 ± 0.30	−3.07 ± 0.29
NM_134372	Acmsd	Rattus norvegicus 2-amino-3-carboxymuconate-6-semialdehyde decarboxylase (acmsd), mRNA	Metabolism	2.50 ± 0.42	2.10 ± 0.21	3.32 ± 0.84	4.04 ± 0.40

Cyanine 5-labeled liver RNA and Cyanine 3-labeled rat common reference RNA were competitively hybridized to microarrays. Hybridization signals were processed into primary expression ratios ([Cyanine 5-intensity obtained from each sample]/[Cyanine 3-intensity obtained from common reference RNA], and normalized (primary expression ratios). The primary expression ratios were converted into $\log_2$ values ($\log_2$ Cyanine-5 intensity/Cyanine-3 intensity) as described in Section 2. $\log_2$ values for each sample were taken an average and calculated S.D.

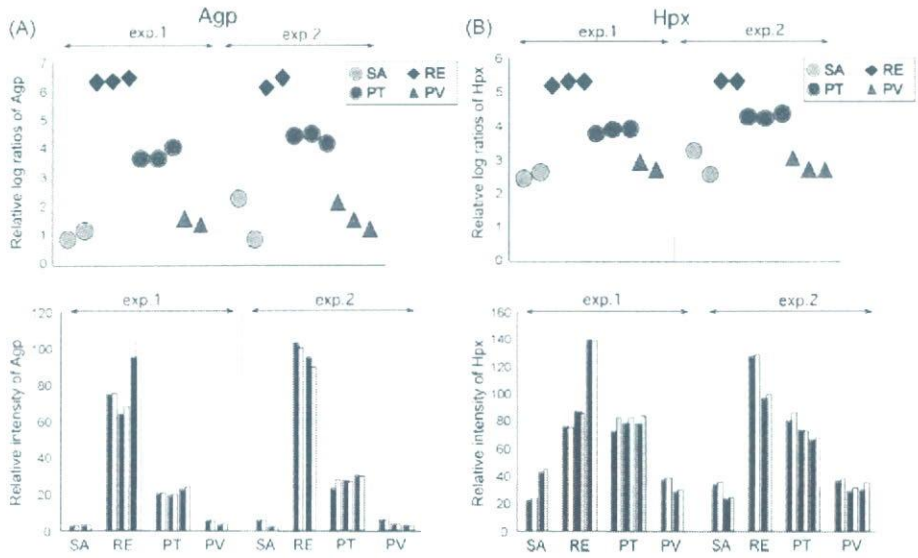

Fig. 4. Comparison of microarray data and quantitative PCR analysis. Expression of Agp (A) and Hpx (B) from DNA microarray analysis (upper panel) is compared with real-time quantitative PCR data (lower panel). (*Upper panels*) Relative $\log_2$ ratios were extracted from the secondary data matrix for Agp and Hpx. Each symbol represents data from individual animals. Two independent experiments in microarray analysis are shown. (*Lower panels*) Quantitative PCR analysis of treated livers from individual animals is shown. Duplicate data from each animal is shown as black and white bars. Agp and Hpx expression was assessed relative to rat β-actin.

concentrations of 5 μg/ml ($P < 0.05$) in comparison with SA, PV, and PT (0.008–0.2 μg/ml). At concentration of 1 μg/ml, some animals showed slight high expression of these genes in comparison with the animals treated with SA, PV or PT (0.008–0.2 μg/ml). These findings suggest that Agp and Hpx may be good candidates to monitor the PT-induced toxicity.

4. Discussion

In this study, we identified genes whose expression is affected by PT-related toxicity using DNA microarray analysis. Although the principle of nucleic acid hybridization is not new, microarrays have opened the way for parallel

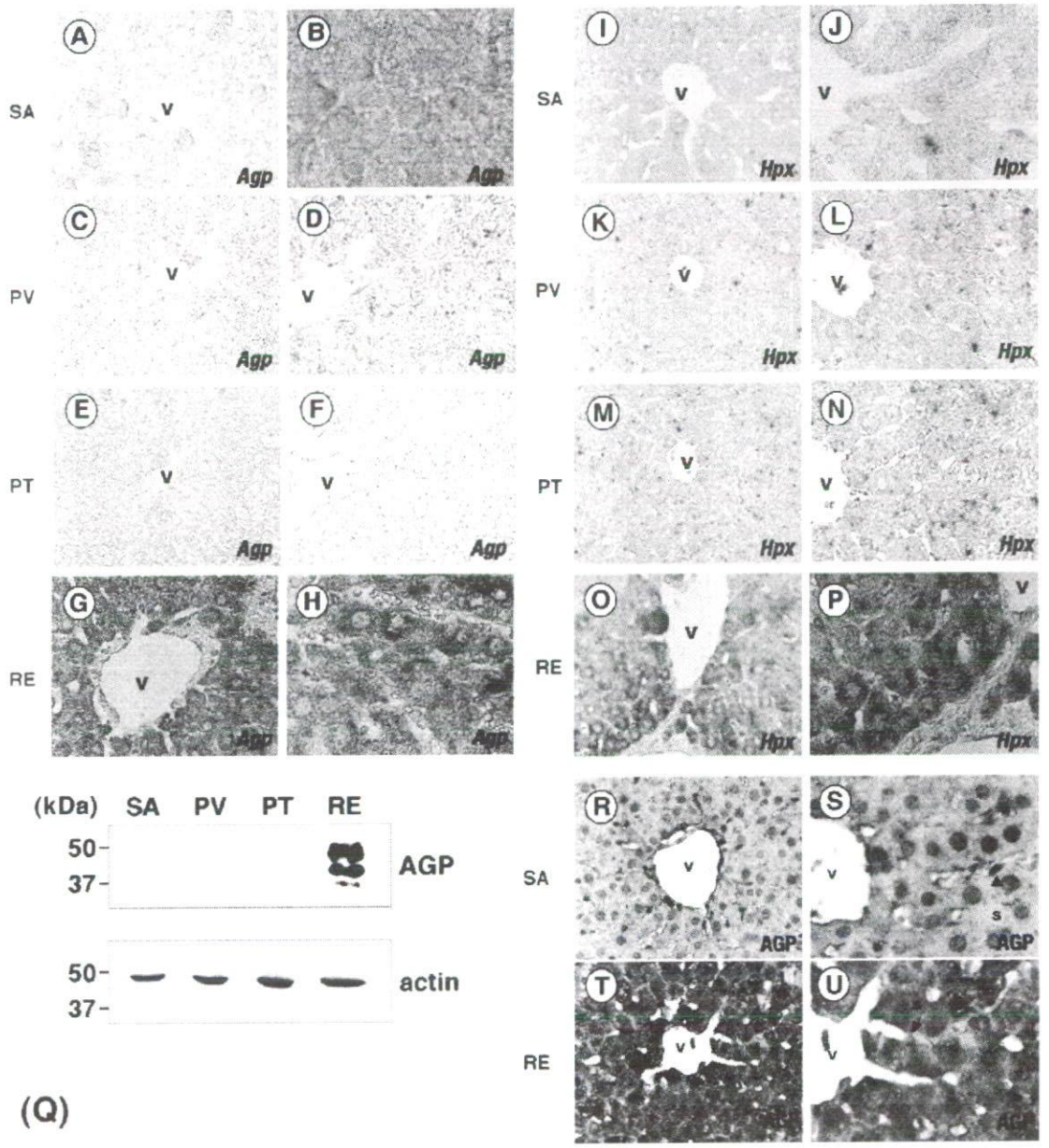

Fig. 5. Expression of Agp and Hpx in RE-, PT-, PV-, and SA-treated liver. Expression of Agp mRNA analyzed by *in situ* hybridization. SA-, PV-, PT-, and RE-treated liver was analyzed at low (A, C, E, and G) and high (B, D, F, and H) magnification. (Q) AGP protein expression in the liver was analyzed by Western blotting. (R–U) Expression of AGP protein in the liver was analyzed by immunohistochemistry. The nuclei were stained with hematoxilin (blue). SA-treated liver was analyzed at low (R) and high (S) magnification. RE-treated liver was analyzed at low (T) and high (U) magnification. Brown indicated AGP protein expression. (I–P) Expression of Hpx mRNA in liver analyzed by *in situ* hybridization. Sections of SA-, PV-, PT-, and RE-treated liver were hybridized with Hpx-specific probes and analyzed at low (I, K, M, and O) and high (J, L, N, and P) magnification. Brown signals represent Hpx expression.

detection and analysis of expression patterns of thousands of genes in a single experiment, and its sensitivity allows detection of subtle differences otherwise difficult to detect. In addition, DNA microarray-based approaches allow us to interrogate toxin-related genomes without bias as to which genes might be altered in expression.

Our histological study showed that RE-treatment severely decreased PAS-stained glycogen granules in hepatocytes. Since hepatocytes are normally full of such granules, their loss suggests a severe load of toxic substances in liver cells [17]. As liver is a major detoxifying organ and analysis of pharmaceutical toxicity using the DNA array has been undertaken in liver [18], we considered liver an appropriate organ to analyze biological alterations with pertussis vaccine.

Based on analysis of 10,490 of rat genes, we identified 150 genes demonstrating significant changes either upward

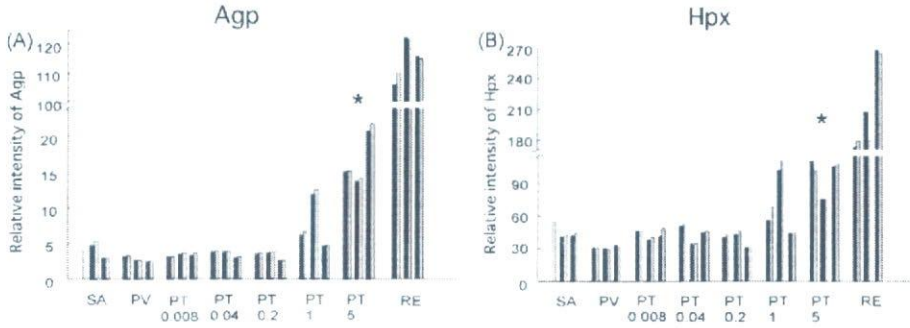

Fig. 6. Quantitative PCR analysis of Agp and Hpx expression in RE-, PT-, PV-, and SA-treated liver. Gene expression of Agp (A) and Hpx (B) in liver treated with various concentrations of PT and RE were analyzed by Q-PCR. Agp and Hpx expression was assessed relative to rat β-actin. Duplicate data from each animal is shown as black and white bars. Three animals per group were analyzed. PT0.008, PT 0.008 μg/ml; PT0.04, PT 0.04 μg/ml; PT0.2, PT 0.2 μg/ml; PT1, PT 1.0 μg/ml; PT5, PT 5.0 μg/ml. Asterisk denotes significant differences ($P < 0.05$) by the Student's *t*-test.

or downward in gene expression after RE-treatment. Among them, several metabolism-relate genes, such as FABP (fatty acid-binding protein; U7558) and NaCT (Na+-coupled citrate transporter; NM_170668) showed the great increase in expression level. FABP participates in the uptake, intracellular metabolism and/or transport of long chain fatty acids. NaCT plays a role in cellular utilization of citrate in blood for the synthesis of fatty acids and cholesterol and for the generation of energy. The great increase of these genes may be correlated to the toxin-related state of starvation that requires urgent energy derived from fatty tissues.

Reduction in PAS-positive glycogen granules in the liver (Fig. 2) after RE-treatment is consistent with this finding. Gordon et al. have reported that toxic substrates induce abnormal PAS-staining in liver cells due to reduced glycogen granules [19]. Inflammation-related genes, such as MIF (U62326), AGP (J00695), and IL-1β (NM_031512) are also up-regulated in RE-treated liver, suggesting that acute inflammation is induced by RE-treatment. In addition, many forms of P450 (NM_19303, M16654, NM_012730, X53477, J02868) are induced in the liver by RE treatment. Comparing gene expression among SA-, PT-, and RE-treated animals, we identified nine genes that were up-regulated in toxic conditions. As shown in Table 1, five genes participated in metabolism, and four genes participated in inflammation. Among them, Agp and Hpx showed unequivocal correlation with RE treatment both in the DNA microarray and histological analysis. AGP is a 41–43 kDa glycoprotein with several activities, such as immunomodulating effects and the ability to bind steroid hormones and other molecules [20,21]. Reportedly, AGP serum concentrations, which remain stable in physiological conditions (about 1 g/l in human and 0.2 g/l in rats), increase several-fold during acute-phase inflammatory reactions and AGP is considered as a major member of the positive acute phase protein family. HPX is a serum glycoprotein with a high affinity for heme, and it is produced by and secreted from the liver. It is also known as a scavenger/transporter of heme [22]. Previous studies indicate that purified HPX is an acute-phase reactant with serum levels increasing several-fold following experimentally induced inflammation [23,24]. These two genes likely react to RE and PT through acute-phase inflammatory reactions. These findings suggest that these biomarkers may be useful to detect PT-induced toxicity in pertussis vaccines.

So far, conventional leukocytosis promoting tests can detect active PT contamination at concentrations greater than 5 μg/ml. While PAS staining of glycogen granules in RE-treated hepatocytes was weak, hepatocytes treated with a high concentration of PT (5 μg/ml) were normally stained with PAS. With our method, we detected Agp and Hpx at a 5 μg/ml PT and the expression level of both genes was dose dependent on PT concentration (Fig. 6). These findings suggest that the gene expression analysis should be useful to detect the PT activity specifically as well as leukocyte-promoting tests. We could detect the different time course of the toxic effects observed as measured by gene expression analysis and leukocytosis. The specific gene expression of Agp and Hpx were observed at day 1 post-treatment, however the increase in WBC were only observed after 2 days. These findings suggest that new test takes the shorter testing period.

Many manufacturers are improving vaccine quality by new methods, such as by using cultured cell lines. However improvements in quality control are continuously required. Since microarray analysis can cover thousands of genes rapidly, it may revolutionize vaccine safety tests and in doing so increase our understanding of molecular mechanisms underlying vaccine toxicity. Given the small variability among test animals, such an approach could potentially reduce the number of animals assayed, alleviating in part ethical problems related to animal tests, which are important issues for regulators worldwide. This method can be used for safety evaluation of different vaccines, such as the emerging vaccine for high pathogenic influenza. So far, safety assessment of vaccines before licensing requires a long time period. Our present assay, with its high reproducibility and reliability, could considerably shorten that period.

Acknowledgments

The authors thank Dr. Hiroshi Yoshikura for helpful discussion and critical reading of the manuscript. The authors have no conflicting financial interests.

Note about research grants: This work was supported by Grants-in-Aid from the Ministry of Health, Labour and Welfare, Japan.

References

[1] Bordet J, Gengou D. Le micrrobe de la coqueluche. Ann Inst Pasteur 1909;23:415–9.
[2] Cone TJ. Whooping cough is first described as a disease suigeneris by Baillou in 1640. Pediatrics 1970;46:522.
[3] Sato H, Sato Y. *Bordetella pertussis* infection in mice: correlation of specific antibodies against two antigens, pertussis toxin, and filamentous hemagglutinin with mouse protectivity in an intracerebral or aerosol challenge system. Infect Immun 1984;46(2):415–21.
[4] Pertussis. In: Atkinson W, Hamborsky J, McIntyre L, Wolfe S, editors. Epidemiology and Prevention of Vaccine-Preventable Diseases. 9th ed. Washington DC: Centers for Disease Control and Prevention; 2006. p. 79–96.
[5] Ministry of Health and Welfare, J.G. The minimum requirements of biological products of Japan 1986. Tokyo: Ministry of Health and Welfare; 1986.
[6] Horiuchi Y, Takahashi M, Konda T, Ochiai M, Yamamoto A, Kataoka M, et al. Quality control of diphtheria tetanus acellular pertussis combined (DTaP) vaccines in Japan. Jpn J Infect Dis 2001;54(5):167–80.
[7] Iwasa S, Ishida S, Asakawa S, Kurokawa M. Lymphocytosis-promoting factor produced by *Bordetella pertussis*. Jpn J Med Sci Biol 1968; 21:363–8.
[8] Morsel S. Studies on the lymphocytosis induced in mice by *Bordetella pertussis*. J Exp Med 1965;121:49–68.
[9] Cyster JG, Goodnow CC. Pertussis toxin inhibits migration of B and T lymphocytes into splenic white pulp cords. J Exp Med 1995;182(2): 581–6.
[10] Ishida S, Kurokawa M, Asakawa S, Iwasa S. A sensitive assay method for the histamine-sensitizing factor using change in rectal temperature of mice after histamine challenge as a response. J Biol Stand 1979;7(1):21–9.
[11] Sakamoto A, Imai J, Nishikawa A, Honma R, Ito E, Yanagisawa Y, et al. Influence of inhalation anesthesia assessed by comprehensive gene expression profiling. Gene 2005;356:39–48.
[12] Ejiri N, Katayama K, Kiyosawa N, Baba Y, Doi K. Microarray analysis on Phase II drug metabolizing enzymes expression in pregnant rats after treatment with pregnenolone-16alpha-carbonitrile or phenobarbital. Exp Mol Pathol 2005;79(3):272–7.
[13] Toyooka Y, Tsunekawa N, Takahashi Y, Matsui Y, Satoh M, Noce T. Expression and intracellular localization of mouse Vasa-homologue protein during germ cell development. Mech Dev 2000;93(1–2): 139–49.
[14] Fujiwara Y, Komiya T, Kawabata H, Sato M, Fujimoto H, Furusawa M, et al. Isolation of a DEAD-family protein gene that encodes a murine homolog of Drosophila vasa and its specific expression in germ cell lineage. Proc Natl Acad Sci USA 1994;91(25):12258–62.
[15] Kobayashi S, Ito E, Honma R, Nojima Y, Shibuya M, Watanabe S, et al. Dynamic regulation of gene expression by the Flt-1 kinase and Matrigel in endothelial tubulogenesis. Genomics 2004;84(1):185–92.
[16] Ito E, Honma R, Imai J, Azuma S, Kanno T, Mori S, et al. A tetraspanin-family protein, T-cell acute lymphoblastic leukemia-associated antigen 1, is induced by the Ewing's sarcoma-Wilms' tumor 1 fusion protein of desmoplastic small round-cell tumor. Am J Pathol 2003;163(6): 2165–72.
[17] Purushotham KR, Lockard VG, Mehendale HM. Amplification of chloroform hepatotoxicity and lethality by dietary chlordecone (kepone) in mice. Toxicol Pathol 1988;16(1):27–34.
[18] Shipkova M, Spielbauer B, Voland A, Grone HJ, Armstrong VW, Oellerich M, et al. cDNA microarray analysis reveals new candidate genes possibly linked to side effects under mycophenolate mofetil therapy. Transplantation 2004;78(8):1145–52.
[19] Gordon GJ, Coleman WB, Hixson DC, Grisham JW. Liver regeneration in rats with retrorsine-induced hepatocellular injury proceeds through a novel cellular response. Am J Pathol 2000;156(2):607–19.
[20] Fournier T, Medjoubi NN, Porquet D. Alpha-1-acid glycoprotein. Biochim Biophys Acta 2000;1482(1–2):157–71.
[21] Nishi K, Sakai N, Komine Y, Maruyama T, Halsall HB, Otagiri M. Structural and drug-binding properties of alpha(1)-acid glycoprotein in reverse micelles. Biochim Biophys Acta 2002;1601(2):185–91.
[22] Tolosano E, Altruda F. Hemopexin: structure, function, and regulation. DNA Cell Biol 2002;21(4):297–306.
[23] Delanghe JR, Langlois MR. Hemopexin: a review of biological aspects and the role in laboratory medicine. Clin Chim Acta 2001;312(1–2): 13–23.
[24] Muller-Eberhard U. Hemopexin. Methods Enzymol 1988;163:536–65.

Ⅴ. 参考資料、その他